On the multi-parameters identification of concrete dams
A novel stochastic inverse approach

Lin, Chaoning; Du, Xiaohu; Chen, Siyu; Li, Tongchun; Zhou, Xinbo; van Gelder, P. H.A.J.M.

DOI
10.1002/nag.3812

Publication date
2024

Document Version
Final published version

Published in
International Journal for Numerical and Analytical Methods in Geomechanics

Received: 31 October 2023 | Revised: 29 June 2024 | Accepted: 5 July 2024

DOI: 10.1002/nag.3812

RESEARCH ARTICLE

WILEY

On the multi-parameters identification of concrete dams: A novel stochastic inverse approach

Chaoning Lin[1] | Xiaohu Du[2] | Siyu Chen[3,4] | Tongchun Li[1] | Xinbo Zhou[2] | P. H. A. J. M. van Gelder[5]

[1]College of Water Conservancy and Hydropower Engineering, Hohai University, Nanjing, China

[2]China Renewable Energy Engineering Institute, Beijing, China

[3]Dam Safety Management Department, Nanjing Hydraulic Research Institute, Nanjing, China

[4]Key Laboratory of Reservoir Dam Safety, Ministry of Water Resources, Nanjing, China

[5]Faculty of Technology, Policy, and Management, Delft University of Technology, Delft, the Netherlands

Correspondence
Siyu Chen, Dam Safety Management Department, Nanjing Hydraulic Research Institute, Nanjing, China.
Email: siyuchen@nhri.cn

Tongchun Li, College of Water Conservancy and Hydropower Engineering, Hohai University, Nanjing, China.
Email: ltchhu@163.com

Funding information
National Key Research and Development Program of China, Grant/Award Number: 2022YFC3005403; National Natural Science Foundation of China, Grant/Award Numbers: 52309151, 52309157; the Open Research Fund of Key Laboratory of Reservoir and Dam Safety Ministry of Water Resources, Grant/Award Number: YK323007; the Science and Technology Project of Power Construction Corporation of China, Grant/Award Number: DJ-HXGG-2022-02

Abstract

This paper introduces a novel stochastic inverse method that utilizes perturbation theory and advanced intelligence techniques to solve the multi-parameter identification problem of concrete dams using displacement field monitoring data. The proposed method considers the uncertainties associated with the dam displacement monitoring data, which are comprised of two distinct sources: the first is related to stochastic mechanical properties of the dam, and the second is due to observation errors. The displacements at different measuring points generated by dam mechanical properties exhibit spatial correlation, while the observation errors at different points can be considered statistically random. In this context, the inversion formulas are derived for unknown stochastic parameters of the dam by combining perturbation equations and Taylor expansion methods. An improved meta-heuristic optimization method is employed to identify the mean of stochastic parameters, while mathematical and statistical methods are used to determine the variance of stochastic parameters. The feasibility of the proposed method is verified through numerical examples of a typical dam section under different conditions. Additionally, the paper discusses and demonstrates the applicability of this method in a practical dam project. Results indicate that this method can effectively capture the uncertainty of dam's mechanical properties and separates them from observation errors.

KEYWORDS

concrete dam, mathematical model, monitoring data, multi-verse optimization, numerical analysis, stochastic inversion

1 INTRODUCTION

Hydropower is the most widely-used renewable power source, accounting for more than 65% of the global power generation capacity from renewable sources. Dams play a crucial role in water conservancy and hydropower projects by providing flood control, power generation, water supply, and irrigation.[1] However, they also pose potential risks to nearby populations, property, and the environment.[2] Past failures, like Malpasset Dam in France and St. Francis Dam in the United States, resulted in enormous loss of life and property.[3,4] Some concrete dams such as Koelnbrein dam in Austria, Dworshak dam in the United States, and Sayano-Shushenskaya dam in Russia had severe cracks and leakage, with tremendously high costs for repair and reinforcement.[5]

Dam surveillance can help reduce the risk of dam failure by early detection of undesirable events.[6,7] Typically, a variety of instruments are placed both inside and outside the dam to monitor external load parameters (such as water level and ambient temperature) and structural response parameters (like displacement and strain).[8–10] Forward analysis methods and inverse analysis methods[11] are two widely-used data analysis approaches which make use of the monitoring data for interpreting the complex dam system.

Forward analysis methods are a fundamental approach for dam safety assessment.[12–14] These methods allow for the estimation of dam response under specific load combinations. Significant progress has been made over the past decades in the development of forward analysis methods for different types of dams.[15,16] The numerous studies carried out in this field can be categorized as physics-based and data-based methods. Physics-based methods use finite element (FE) methods or other numerical techniques to analyze and predict the dam effect field based on provided structural morphology and mechanical parameters. In contrast, data-based methods construct a mathematical monitoring model based on information obtained from prototype observations, which allows for the determination of expected responses using previously collected data.[17]

Inverse analysis methods, also known as system identification, are a powerful tool for determining unknown mechanical parameters, boundaries, or initial conditions.[18–20] Depending on the type of measured data, inverse analysis methods can be subdivided into three categories: stress-based, displacement-based, and hybrid methods.[21] Among these, the displacement-based method has been extensively implemented because the information is easier to obtain. In terms of the solution process, inverse analysis methods can be subdivided into two main categories: direct and indirect methods. The direct inverse analysis method requires the establishment or derivation of explicit equations between mechanical parameters and field monitoring data.[22] The indirect method converts the inversion problem into an optimization problem of an objective function, which is more flexible in generating a solution for nonlinear systems.

This paper focuses on the parameter identification problems of concrete dams. The elastic modulus is an important mechanical parameter for assessing the stiffness and performance of the dam body and foundation.[23] Inverse analysis methods are widely employed to determine the elastic moduli of concrete dams using deformation monitoring data. Sortis et al.[24] presented an identification algorithm for the physical parameters of the hollow gravity dams allowing a useful determination of their equivalent elastic moduli. Yang et al. developed an improved particle swarm optimization (PSO) algorithm to identify the elastic moduli of a concrete dam.[25] Kang et al. proposed a novel multi-parameter inverse analysis approach utilizing a kernel extreme learning machine-based response surface model to identify the elastic moduli of concrete dams.[26]

Current studies on inverse analysis of concrete dams are mainly focused on deterministic mathematical models. Concrete dams are inherently uncertain system, with mechanical parameters that exhibit stochastic behavior due to the variability in material properties, construction quality, and other factors.[27,28] In other structural engineering domains, probability methods have been used to solve inversion and parameter identification problems. The Bayesian approach is one of the most popular methods for solving uncertainty inversion problems,[29,30] typically using Markov chain Monte Carlo (MCMC) methods to determine probability distributions. However, for multi-parameter identification problems of large-scale concrete dams, the MCMC steps require forward FE analysis that is computationally inefficient. The interval inversion algorithm is another useful tool for conducting uncertainty inverse analysis,[31] but its limitation is that the uncertainty of parameters can only be roughly represented by lower and upper bounds, without providing a deeper insight into the essence of the uncertainty.

Perturbation method is an efficient approach for evaluating the uncertainty of structural responses. It involves first- or second-order Taylor series expansions of the governing equations, characterizing the structural behavior by considering terms around the mean values of the fundamental random variables.[32,33] Perturbation method is used in a wide range of fields and has the advantages of computational efficiency, flexibility in handling uncertainties, and interpretability of results.[34] Many studies have applied the perturbation method to address direct problems.[35–37] However, the inverse problem for structures with uncertain parameters has received less attention and only few contributions are available in literature.[38]

For concrete dams, the uncertainties associated with the displacement monitoring data is comprised of two distinct factors: the first is related to stochastic mechanical properties of the dam, and the second is due to observation errors. The displacements at different measuring points generated by dam mechanical properties exhibit spatial correlation due to the common environmental loads they are subjected to, while the observation errors at different points can be considered statistically random.

Upon reflecting on this situation, a novel stochastic inverse method is proposed by combining perturbation theory and advanced meta-heuristic optimization technique. The inversion formulas for unknown mechanical parameters are derived based on multi-point displacement monitoring data, enabling the identification of the mean and variance of the dam's mechanical parameters. Furthermore, this method can effectively separate the perturbed displacements caused by dam mechanical parameters from those caused by observation errors. The proposed inverse method has the advantages of simplicity for formulation, efficiency of execution, and ease of understanding.

This paper is structured into six sections as follows. In Section 2, the derivation process of the stochastic inverse analysis is illustrated in detail. In Section 3, the improved parallel multi-verse optimization (IMVO) is introduced, and the inversion framework is established. Section 4 presents a series of numerical examples of a typical gravity dam section to verify the feasibility of the proposed inverse method. In Section 5, the applicability of the proposed inverse method in practical dam projects is discussed and demonstrated. Finally, the conclusions are provided in Section 6.

2 | STOCHASTIC INVERSE METHOD FOR DAM PARAMETER IDENTIFICATION

When dealing with the parameter identification problem of concrete dam system, it is important to consider the uncertainties associated with two main factors: (1) the uncertainty of material mechanical parameters, and (2) the uncertainty of observation errors. In this section, we derive formulas for solving stochastic mechanical parameters of the dam system based on displacement field monitoring data.

2.1 | Mathematical model

The stochastic parameters (i.e., unknown elastic moduli) of the dam with mean values and perturbation terms are defined in Equation (1):

$$X = \overline{X} + \varepsilon_X, \tag{1}$$

where X represents the vector of stochastic parameters such that $X = \{x_1, x_2, \cdots x_p\}^T$; $\overline{X}$ represents the vector of mean values of stochastic parameters such that $\overline{X} = \{\bar{x}_1, \bar{x}_2, \cdots \bar{x}_p\}^T$; ε_X represents the vector of perturbation terms of stochastic parameters such that $\varepsilon_X = \{\varepsilon_{x_1}, \varepsilon_{x_2}, \cdots \varepsilon_{x_p}\}^T$; and p is the number of stochastic parameters.

It is assumed in this study that the vector of dependent variables, denoted by $\delta(X, Y)$, represents the dam monitoring displacements. Here, X represents a set of unknown stochastic parameters (independent variables), while Y represents a set of environmental parameters such as water level and temperature. Considering the monitoring displacement series $\delta(X, Y)$ as a non-stationary stochastic process with a deterministic trend, it can be expressed as follows:

$$\delta(X, Y) = \bar{\delta}(X, Y) + \varepsilon_\delta, \tag{2}$$

where $\bar{\delta}(X, Y)$ represents the vector of mean values of dam displacements; and ε_δ represents the vector of perturbation terms of dam displacements.

The perturbation terms of dam displacements ε_δ can be decomposed into two parts: $\varepsilon_{\delta X}$ and ε_f. Here, $\varepsilon_{\delta X}$ indicates the displacement perturbation term caused by stochastic parameters, and ε_f represents the displacement perturbation term due to observation errors. The observation errors are independent at each measuring point and follow a normal distribution with a mean of zero.

It is assumed that there are N measuring points, and each point has M groups of displacement monitoring data. According to Equation (2), the variance of the dam displacement at the jth measuring point is formulated as follows:

$$\mathrm{var}(\delta_j) = \frac{1}{M}\sum_{k=1}^{M}(\varepsilon_{\delta_{jk}})^2 = \frac{1}{M}\sum_{k=1}^{M}[\delta(X, Y_{jk}) - \bar{\delta}(X, Y_{jk})]^2, \tag{3}$$

where var denotes the variance operator, and $\delta(X, Y_{jk})$ represents the kth displacement value at the jth measuring point ($j = 1, 2, \cdots, N$ and $k = 1, 2, \cdots, M$). For simplicity, it is defined that $\delta_{jk} = \delta(X, Y_{jk})$, $\bar{\delta}_{jk} = \bar{\delta}_{jk}(X, Y_{jk})$, and $\bar{\delta}_{jk}$ represents the mean value of δ_{jk}.

Suppose that $\delta(X, Y)$ can be expanded into a Taylor series around its mean point. If we exclude the higher-order polynomial terms and only retain the first-order polynomial term, then we obtain:

$$\delta(X, Y) = \delta(\overline{X}, Y) + \sum \left.\frac{\partial \delta}{\partial x}\right|_{X=\bar{X}}(X - \overline{X}) = \delta(\overline{X}, Y) + \sum \left.\frac{\partial \delta}{\partial x}\right|_{X=\bar{X}} \varepsilon_X. \tag{4}$$

The following formula gives the mean value of Equation (4):

$$\mathrm{E}(\delta(X,Y)) = \bar{\delta}(X,Y) = \delta(\overline{X},Y), \tag{5}$$

where E denotes the mathematical expectation.

Substituting Equation (5) into Equation (3), the expression turns out to be:

$$\mathrm{var}(\delta_j) = \frac{1}{M}\sum_{k=1}^{M}[\delta(X, Y_{jk}) - \bar{\delta}(X, Y_{jk})]^2 = \frac{1}{M}\sum_{k=1}^{M}[\delta(X, Y_{jk}) - \delta(\overline{X}, Y_{jk})]^2. \tag{6}$$

2.2 | Derivation of parameter mean and variance

Define the objective function as follows:

$$J = \mathrm{var}(\delta) = \frac{1}{N}\sum_{j=1}^{N}\mathrm{var}(\delta_j) = \frac{1}{M \times N}\sum_{j=1}^{M}\sum_{k=1}^{N}[\delta(X, Y_{jk}) - \delta(\overline{X}, Y_{jk})]^2, \tag{7}$$

where $\delta(\overline{X}, Y)$ represents the calculated displacement obtained by taking the mean value of X.

Based on this, we can estimate the mean value of the stochastic parameter by minimizing the objective function. The formula for solving the variance of the stochastic parameter is derived below.

For a certain monitoring moment $k(k = 1, 2, \cdots, M)$, we define:

$$B(\overline{X}, Y_k) = \left.\frac{\partial \delta}{\partial X}\right|_{k,X=\bar{X}} = \begin{bmatrix} \frac{\partial \delta_1}{\partial x_1} & \frac{\partial \delta_1}{\partial x_2} & \cdots & \frac{\partial \delta_1}{\partial x_p} \\ \frac{\partial \delta_2}{\partial x_1} & \frac{\partial \delta_2}{\partial x_2} & \cdots & \frac{\partial \delta_2}{\partial x_p} \\ \cdots & \cdots & \cdots & \cdots \\ \frac{\partial \delta_N}{\partial x_1} & \frac{\partial \delta_N}{\partial x_2} & \cdots & \frac{\partial \delta_N}{\partial x_p} \end{bmatrix}_{k,X=\bar{X}}, \tag{8}$$

where $B(\overline{X}, Y_k) \in R^{N\times p}$ is the sensitivity coefficient; N is the number of measuring points; and p is the number of stochastic parameters.

Then Equation (4) can be rewritten as follows:

$$\delta(X, Y_k) = \delta(\overline{X}, Y_k) + B(\overline{X}, Y_k)\{\varepsilon_{Xk}\}, \tag{9}$$

where $\delta(X, Y_k)$ is an $N \times 1$ vector; and $\{\varepsilon_{Xk}\}$ is a $p \times 1$ vector such that $\{\varepsilon_{Xk}\} = \{\varepsilon_{x_1k}\ \varepsilon_{x_2k}\ \cdots\ \varepsilon_{x_pk}\}^T$.

Equation (9) can be transformed into:

$$B(\overline{X}, Y_k)\{\varepsilon_{Xk}\} = \delta(X, Y_k) - \delta(\overline{X}, Y_k). \tag{10}$$

Multiplying both sides of Equation (10) with $B(\overline{X}, Y_k)^T$, we obtain:

$$B(\overline{X}, Y_k)^T B(\overline{X}, Y_k)\{\varepsilon_{Xk}\} = B(\overline{X}, Y_k)^T\{\delta(X, Y_k) - \delta(\overline{X}, Y_k)\}. \tag{11}$$

Then the solution turns out to be:

$$\{\varepsilon_{Xk}\} = \left[B(\overline{X}, Y_k)^T B(\overline{X}, Y_k)\right]^{-1} B(\overline{X}, Y_k)^T\{\delta(X, Y_k) - \delta(\overline{X}, Y_k)\}. \tag{12}$$

If the number of equations is greater than the unknown variables, the solution of the redundant equations is equal to the least-squares solution.

Hence, the variance of the stochastic parameter can be obtained:

$$\mathrm{var}(\varepsilon_X) = \left\{\sigma_X^2\right\} = \left\{\sigma_{x_1}^2 \quad \sigma_{x_2}^2 \cdots \quad \sigma_{x_P}^2\right\}^T = \frac{1}{M}\left\{\sum_{k=1}^{M}\left\{\varepsilon_{x_1k}\right\}^2 \quad \sum_{k=1}^{M}\left\{\varepsilon_{x_2k}\right\}^2 \quad \cdots \quad \sum_{k=1}^{M}\left\{\varepsilon_{x_pk}\right\}^2\right\}^T. \tag{13}$$

Substituting the calculation results of Equation (12) into Equation (10), the displacement perturbation term caused by ε_X at the moment k is given by:

$$\{\varepsilon_{\delta Xk}\} = B(\overline{X}, Y_k)\{\varepsilon_{Xk}\}, \tag{14}$$

where $\{\varepsilon_{\delta Xk}\}$ is an $N \times 1$ vector.

As described in Equation (2), the perturbation term of the dam displacement is composed of two parts. The observation error at the moment k is given by:

$$\left\{\varepsilon_{fk}\right\} = \left\{\varepsilon_{\delta k}\right\} - \left\{\varepsilon_{\delta Xk}\right\}. \tag{15}$$

According to Equations (14) and (15), we can obtain the variance of the two displacement perturbation terms ($\mathrm{var}(\delta_X)$ and $\mathrm{var}(\delta_f)$).

2.3 | Formula of sensitivity coefficients

Discretizing the continuous dam structure into a FE framework, the FE equations related to nodal displacements δ and nodal loads F takes the following form:

$$K\delta = F. \tag{16}$$

The global stiffness matrix K of the structure is given as follows:

$$K = \int_V B^{\mathrm{T}} D B dV, \tag{17}$$

where D indicates the elastic stress-strain matrix expressed by elastic constants including elastic modulus and Poisson ratio; and B indicates the strain-displacement matrix that describes the geometric properties of the elements.

It can be inferred from Equation (16) that:

$$\overline{K\delta} = \overline{F}. \tag{18}$$

Assuming that the elastic moduli are stochastic parameters, the formula for the first derivative of Equation (16) at the mean point is given by:

$$\overline{K}\left.\frac{\partial\delta}{\partial X}\right|_{X=\bar{X}} + \left.\frac{\partial K}{\partial X}\right|_{X=\bar{X}}\bar{\delta} = \frac{\partial F}{\partial X}. \tag{19}$$

Equation (19) can be rewritten as follows:

$$\overline{K}\left.\frac{\partial\delta}{\partial X}\right|_{X=\bar{X}} = \frac{\partial F}{\partial X} - \left.\frac{\partial K}{\partial X}\right|_{X=\bar{X}}\bar{\delta}. \tag{20}$$

The gradient vector $B(\overline{X}, Y)$ is also referred to as the sensitivity coefficient. Since the gradient vector of the displacement with respect to stochastic parameters does not have an explicit analytic expression, the central difference method is adopted to solve it, and the component $b_{ji}(\overline{X}, Y_k)$ in the matrix $B(\overline{X}, Y_k)$ can be formulated as follows:

$$b_{ji}(\overline{X}, Y_k) = \left.\frac{\partial\delta_j}{\partial x_i}\right|_{k,X=\overline{X}} = \frac{\delta(\bar{x}_1, \cdots, \bar{x}_i + \Delta x_i, \cdots, \bar{x}_p, Y_k) - \delta(\bar{x}_1, \cdots, \bar{x}_i - \Delta x_i, \cdots, \bar{x}_p, Y_k)}{2\Delta x_i}, \tag{21}$$

where $j = 1, 2, \cdots, N$ and $i = 1, 2, \cdots, p$.

The aforementioned formula for the sensitivity coefficient is based on choosing a reference Δx_i, which is generally suggested within the range of:

$$\Delta x_i = \alpha x_i, \ \ 10^{-5} \le \alpha \le 10^{-2}. \tag{22}$$

The value of α is set as 0.001 in this study.

3 | INVERSE ANALYSIS FRAMEWORK FOR PARAMETER IDENTIFICATION

In this section, the inverse analysis framework for parameter identification is introduced. The multi-verse optimization (MVO) is employed and improved for identifying the mean of stochastic parameters, while mathematical and statistical methods are used to determine the variance of stochastic parameters.

3.1 | Improved parallel multi-verse optimization (IMVO)

A forefront optimization algorithm called MVO[39] is studied and applied in inverse analysis framework. The main inspirations of this algorithm are based on three concepts in cosmology: white hole, black hole, and wormhole. MVO shares some advantages with other meta-heuristic optimization algorithms, such as simplicity and speed in searching. Furthermore, it has a unique advantage that it has only two hyper-parameters responsible for balancing between exploration and exploitation.[40]

In MVO, a solution (unknown elastic moduli) is represented by a universe, where each variable corresponds to an object in the universe. The fitness value of the solution (i.e., the value of the objective function) is indicated by the inflation rate of the universe. The population of universes U is defined as follows:

$$U = \begin{bmatrix} x_1^1 & x_1^2 & \cdots & x_1^d \\ x_2 & x_2^2 & \cdots & x_2^d \\ \cdots & \cdots & \cdots & \cdots \\ x_n^1 & x_n^2 & \cdots & x_n^d \end{bmatrix}, \tag{23}$$

where d is the number of objects (variables) and n is the number of universes (candidate solutions).

The main mathematical model of this algorithm is based on Equations (24) and (25), which are described as follows:

$$x_i^j = \begin{cases} x_k^j, & r_1 < NI(U_i) \\ x_i^j, & r_1 \geq NI(U_i) \end{cases}, \tag{24}$$

where x_i^j represents the jth variable of the ith universe; x_k^j represents the jth variable of the kth universe which selected by a roulette wheel selection mechanism; U_i denotes the ith universe and $NI(U_i)$ is the normalized inflation rate (fitness value) of the U_i; r_1 is a random number in the range of [0,1].

The evolution of universes also follows:

$$x_i^j = \begin{cases} \begin{cases} X_j + \mathrm{T}DR * ((ub_j - lb_j) * r_4 + lb_j), \ r_3 < 0.5 \\ X_j - \mathrm{TDR} * ((ub_j - lb_j) * r_4 + lb_j), \ r_3 \geq 0.5 \end{cases} & r_2 < \mathrm{WEP} \\ \quad x_i^j \qquad\qquad\qquad\qquad r_2 \geq \mathrm{WEP} \end{cases}, \tag{25}$$

where X_j denotes the jth variables of the best universe formed so far; lb_j and ub_j denote the lower and upper boundaries of the jth variable; r_2, r_3 and r_4 are random numbers in the range of [0,1].

There are two adaptive coefficients in the MVO: the wormhole existence probability (WEP) and the traveling distance rate (TDR).[39] WEP increases over the iterations in order to emphasize exploitation as the progress of optimization process. TDR is increased over the iterations to have more precise exploitation/local search around the best solution obtained so far. The expressions are as follows:

$$\mathrm{WEP} = \mathrm{WEP}_{\min} + l * \left(\frac{\mathrm{WEP}_{\max} - \mathrm{WEP}_{\min}}{L}\right), \tag{26}$$

$$\mathrm{TDR} = 1 - \frac{l^{1/q}}{L^{1/q}}, \tag{27}$$

where $\mathrm{WEP}_{\min}$ is the minimum value which is ordinarily set to 0.2; $\mathrm{WEP}_{\max}$ is the maximum value which is ordinarily set to 1; l and L represent the current iteration number and the maximum iteration number; q indicates the exploitation factor which is ordinarily set to 6.

In the past few years, a number of variants[41] were proposed to improve the performance of MVO that include the Chaotic MVO,[42] memory-assisted adaptive MVO,[43] hybridized version of MVO with genetic algorithm (GA),[44] hybridized version of MVO with grey wolf optimizer (GWO),[45] and so on.

For the parameter inversion problem in dam engineering, the convergence process has nonlinear characteristics. To improve the searching ability of the basic MVO algorithm, this paper presents a nonlinear formula for WEP, as expressed in Equation (28). The adjusted WEP grows faster during iterations, which can enhance the exploitation in the optimization process. Figure 1 illustrates the nonlinear increasing process of the improved WEP over a maximum iteration number of 50.

$$\mathrm{WEP} = \mathrm{WEP}_{\min} + \left(\frac{\mathrm{WEP}_{\max} - \mathrm{WEP}_{\min}}{1 - (5e)^{-1}}\right) \times (1 - (5e)^{-\frac{l}{L}}), \tag{28}$$

where e is the base of the natural logarithm.

Moreover, this paper introduces multi-core parallel computing to speed up the optimization process for large-scale numerical analysis problems. In the proposed IMVO, universes are divided into subpopulations for parallelization via a spatially structured network, allowing subpopulations to evolve on different processors while exchanging good solutions.

3.2 | Statistical model of dam monitoring displacement

Statistical models are often employed to find out the contribution of external loads (such as water pressure and temperature) to dam deformation.[46] An analytical formula gives the along-river displacement of a concrete dam as the sum of

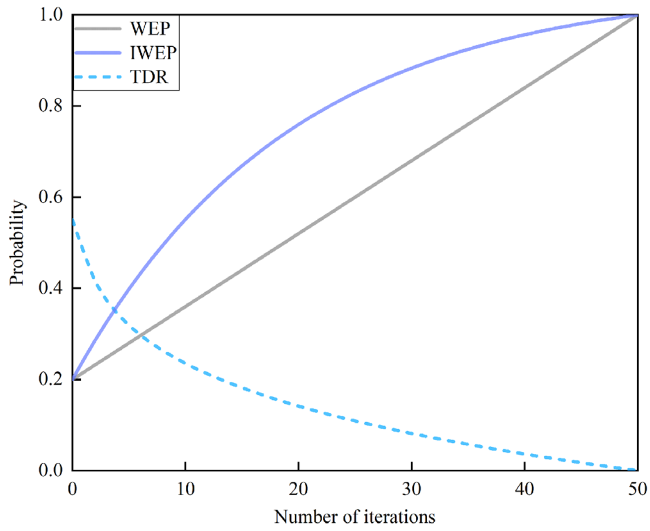

FIGURE 1 Improved wormhole existence probability (IWEP) and traveling distance rate (TDR).

three terms[47]:

$$u = u_H + u_T + u_\theta, \tag{29}$$

where u denotes the along-river displacement; u_H denotes the hydraulic component; u_T denotes the thermal component; and u_θ denotes the irreversible component.

The hydraulic component can be described using a polynomial function depending on the reservoir water level as follows:

$$u_H = \sum_i^m a_i H^i, \tag{30}$$

where $a_1 \sim a_3$ are regression coefficients of the hydraulic component; H is the upstream water level; and the value of m depends on the dam type and $m = 3$ is suitable for the gravity dam.

The thermal component can be expressed by a combination of harmonic functions as follows[48]:

$$u_T = \sum_i^2 (b_{1i} \sin(i\omega) + b_{2i} \cos(i\omega)), \tag{31}$$

where b_{11}, b_{12}, b_{21}, and b_{21} are regression coefficients of the thermal component; $\omega = \pi t/365$ and t is the number of days from the initial date.

The irreversible component reflects the irreversible deformation of the dam in a certain direction over time. According to previous research results, the irreversible component can be described by a polynomial function consisting of linear, exponential, logarithmic, and hyperbolic functions,[49] shown as follows:

$$u_\theta = \sum_i^4 c_i F_i, \tag{32}$$

$$F_1 = \theta,\ \ F_2 = 1 - e^{-\theta},\ F_3 = \ln(\theta + 1),\ \ F_4 = \theta/(\theta + 1), \tag{33}$$

where $c_1 \sim c_4$ are regression coefficients of the irreversible component; θ is the time calculation parameter related to t, which can be expressed as $\theta = t/100$.

The coefficients $(a_1, a_2, \ldots c_4)$ can be calculated using multiple linear regression analysis. The deformation caused by hydrostatic pressure is primarily associated with elastic moduli. By subtracting the thermal and irreversible components

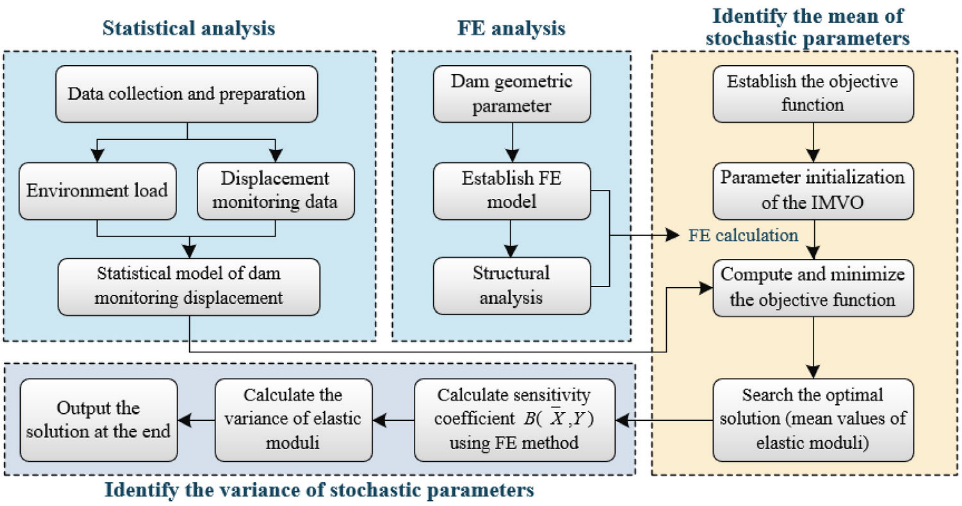

FIGURE 2 Flowchart of the stochastic inverse method for dam elastic moduli.

from the total displacement u, the hydraulic component u_H can be obtained as follows:

$$u_H = u - u_T - u_\theta. \tag{34}$$

3.3 | Inverse problem formulation and solution strategies

The flowchart of the stochastic inverse method is illustrated in Figure 2. The process involves the following steps:

Step 1. Collect monitoring data from the dam surveillance system.
Step 2. Establish the statistical model of dam displacement and isolate the hydraulic component from the total displacement.
Step 3. Establish the FE model of the dam and calculate the dam displacement field under the given load combination.
Step 4. Establish the objective function (Equation 7) of the inverse problem. Set the parameter intervals, the population size and the termination conditions. Search the optimal solution (i.e., the mean values of elastic moduli) of the objective function using IMVO.
Step 5. Calculate the first-order sensitivity coefficient $B(\overline{X}, Y)$ using FE method and the variance of elastic moduli according to Equations (12) and (13).
Step 6. Output the solution at the end.

4 | METHOD VALIDATION

In this section, numerical examples are conducted to verify the feasibility of the stochastic inverse method and the computational efficiency of the inverse analysis framework based on the IMVO algorithm.

4.1 | Analysis procedure

Based on the dam displacement field monitoring data, the proposed stochastic inverse method can capture the uncertainty of the dam's mechanical properties and separate them from observation errors. Numerical examples are conducted on a typical gravity dam section to demonstrate the feasibility of the inverse method when dealing with multiple stochastic parameters and different measuring points. The main steps of the procedure are as follows:

Step 1. Establish the FE model of the dam section.

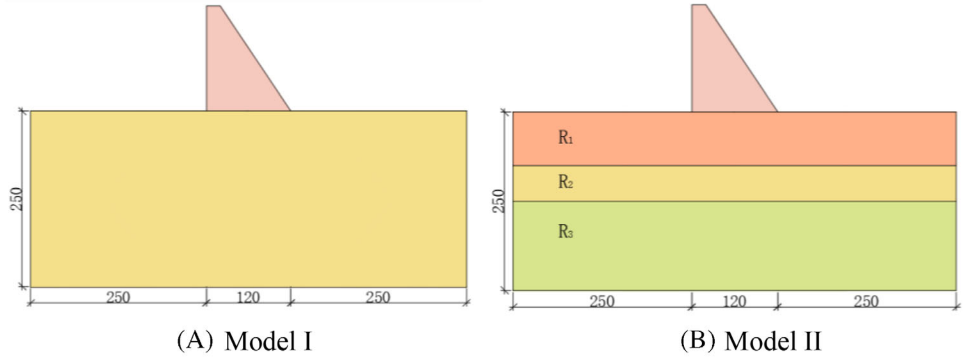

FIGURE 3 Example models.

Step 2. Determine the number of stochastic parameters. Set the mean, variance, and distribution of stochastic parameters, as well as observation errors.
Step 3. Randomly generate a series of independent samples of stochastic parameters and observation errors.
Step 4. Use the FE model to calculate the dam displacement for different parameter samples under given hydrostatic loads.
Step 5. Assume the calculated displacement including observation errors represents the observations at each measuring point.
Step 6. Identify the mean of stochastic parameters by using the IMVO according to Equation (7), and identify the variance of stochastic parameters according to Equation (13).
Step 7. Compare the inversion results with the theoretical values, and analyze the feasibility of the proposed stochastic inverse method.

4.2 | Case study

Two typical gravity dam models are established with a dam height of 150 m, as shown in Figure 3. In Model I, the elastic modulus of the dam body is assumed to follow a normal distribution with a mean of 30 GPa and a standard deviation of 4 GPa. The elastic modulus of the dam foundation is assumed to follow a normal distribution with a mean of 20 GPa and a standard deviation of 4 GPa. In Model II, the dam body maintains the same parameter settings as Model I. The dam foundation is divided into three layers (R_1, R_2, and R_3), each with different mean values of elastic moduli (15, 20, and 25 GPa) and corresponding standard deviations (3, 4, and 5 GPa). Further, it is assumed that observation errors follow a normal distribution with a mean of zero and a standard deviation of 1.00 mm.

The displacement monitoring instruments, such as pendulums, are typically located in transversal and vertical galleries near the upstream surface of gravity dams. According to the current measuring point arrangements, the instruments are assumed to be equipped at points D_1-D_7 for monitoring the along-river displacement of the dam. The corresponding nodes of the measuring points are depicted in Figure 4. To analyze the applicability of the proposed inverse method for different numbers of measuring points, two groups of measuring point arrangements are selected: (i) all seven points (D_1-D_7) have observations and (ii) only four points (D_1, D_3, D_5, and D_7) have observations.

In addition, two different load conditions are analyzed and compared in case study. The first condition requires maintaining a constant water level of 140 m throughout the study. The second condition involves randomly changing the water level between 120 and 150 m at each moment. The eight examples are listed in Table 1.

4.3 | Results and discussion

The proposed inverse analysis framework is applied to the eight examples. For each example, 500 groups of parameter samples are generated. The inversion results are presented in Table 1, where E_c' and σ_c' represent the identified mean and standard deviation of the elastic modulus of the dam body, and E_r' (or E_{r1}', E_{r2}', E_{r3}') and σ_r' (or σ_{r1}', σ_{r2}', σ_{r3}') represent the identified mean and standard deviation of the elastic modulus of the foundation.

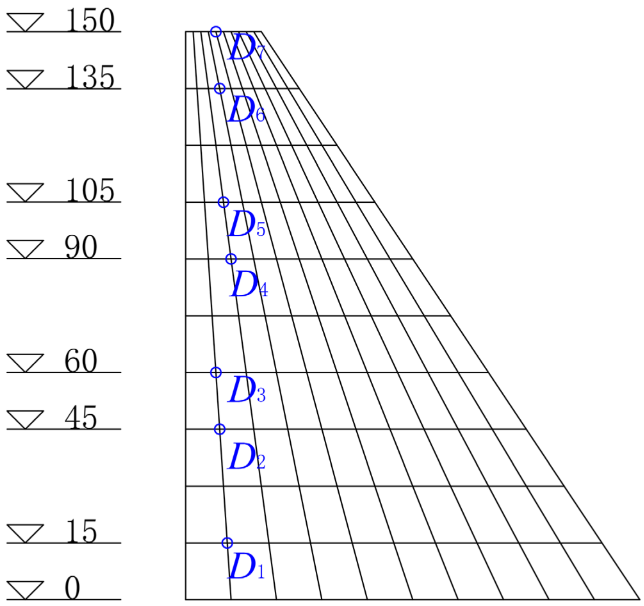

FIGURE 4 Schematic diagram of measuring points (heights are in meters).

TABLE 1 The examples and results.

Example	Model	Measuring arrangement	Water level (m)	Inversion results, the mean and standard deviation (GPa)			
				E'_c	σ'_c	E'_r (E'_{r1}, E'_{r2}, E'_{r3})	σ'_r (σ'_{r1}, σ'_{r2}, σ'_{r3})
(1)	I	i	140	29.76	4.46	19.83	4.06
(2)	I	i	120–150	29.80	4.34	19.77	4.27
(3)	I	ii	140	29.76	4.75	19.78	4.68
(4)	I	ii	120–150	29.72	4.86	19.80	4.75
(5)	II	i	140 m	30.11	4.21	14.75, 19.88, 24.63	3.43, 4.35, 5.38
(6)	II	i	120–150	29.56	4.34	14.84, 20.14, 24.84	3.40, 3.89, 5.54
(7)	II	ii	140	30.41	4.87	14.78, 19.87, 25.35	4.02, 4.76, 5.82
(8)	II	ii	120-–150	29.43	5.01	14.84, 20.14, 24.84	3.89, 4.92, 6.12

Note: Subscript c refers to dam body and r to dam foundation.

4.3.1 | Feasibility analysis of the stochastic inverse method

After analyzing the results of all eight examples, we take the results of Example (1) for detailed analysis. Figure 5 shows the comparison of the probability density curve between the example samples and the inversion results. It can be seen that the identified mean of the elastic modulus is similar to that of the samples, and the distribution range of the inversion results is slightly wider than that of the samples.

Based on the parameters identified, the displacements of measuring points are calculated and compared with the theoretical values of samples. The statistical results are listed in Table 2. The Columns 2–4 are the sample statistic: $\delta(\overline{X}, Y)$ represents the mean displacement, std(δ_X) represents the standard deviation of the displacement perturbation caused by stochastic mechanical parameters, and std(δ_f) represents the standard deviation of the observation errors. The Columns 5–7 are the statistical results of the inverse analysis: $\delta(\overline{X'}, Y)$ represents the estimated mean displacement calculated based on the mean value of identified parameters, and std(δ'_X) and std(δ'_f) are calculated according to Equations (14) and (15). Results show that the estimated mean displacement is close to that of the samples, and the displacement perturbation caused by stochastic parameters increases with elevation. In addition, the estimated standard deviation of observation errors is approximate to the set value of 1.00 mm. Therefore, the proposed stochastic inverse method can reasonably reveal the uncertainty of dam's elastic properties and separate perturbed displacements generated by stochastic parameters from those attributable to observation errors.

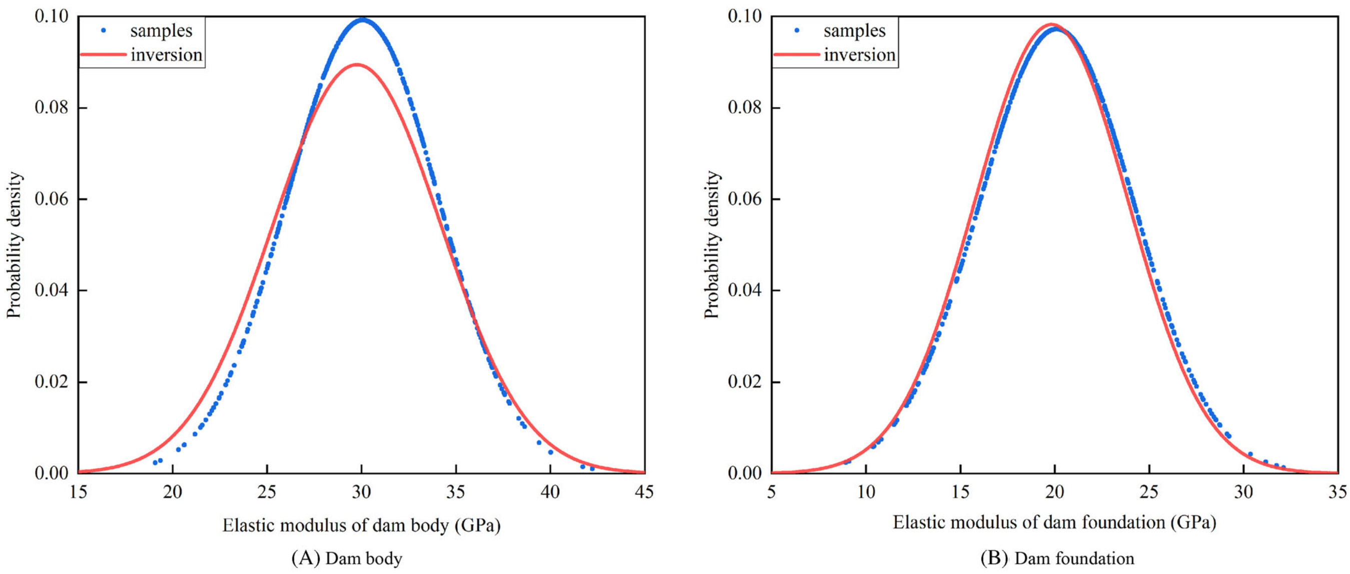

FIGURE 5 Probability density curves of elastic moduli.

TABLE 2 Comparison of samples and estimated results at different measurement points.

	Samples			Estimated results		
Point	$\delta(\overline{X}, Y)$**(mm)**	**std**(δ_X) **(mm)**	**std**(δ_f) **(mm)**	$\delta(\overline{X'}, Y)$**(mm)**	**std**(δ'_X) **(mm)**	**std**(δ'_f) **(mm)**
D_1	9.19	1.79	1.02	9.26	1.66	1.08
D_2	14.50	2.37	0.99	14.62	2.39	1.00
D_3	16.92	2.67	0.98	17.06	2.86	0.97
D_4	21.70	3.26	1.01	21.88	3.38	0.99
D_5	24.20	3.57	1.00	24.40	3.53	1.07
D_6	29.12	4.19	0.99	29.37	4.32	0.97
D_7	31.58	4.49	1.03	31.84	4.66	1.06

For all eight examples, it can be seen from Table 1 that the results obtained by the stochastic inverse method are close to the actual situation and can meet the accuracy requirements. In addition, it can be concluded from the results that increasing the number of measuring points is helpful to improve the accuracy of the inversion results.

4.3.2 | Performance evaluation of the inverse analysis framework based on IMVO

The most computationally intensive part of the inverse analysis framework is the identification of the mean value of the stochastic parameters, as it requires iterative analyzes of the FE model. In order to evaluate the performance of the proposed inverse analysis framework based on IMVO, it is compared with several other inversion optimization algorithms, such as basic MVO, PSO, and GA. According to the trial and experience, the control parameters for each algorithm are set as follows: the population size is taken as 20 and the maximum number of iterations is taken as 50. The WEP in IMVO increases nonlinearly from 0.2 to 1.0 over the course of iterations, while it increases linearly in MVO. The acceleration factors in the PSO are set to $c_1 = c_2 = 0.5$ and the inertia weight is taken as $\omega = 0.9$. In GA, the crossover rate and mutation rate are set to $P_c = 0.2$ and $P_m = 0.5$, respectively.

After conducting a detailed analysis, we take the results of Examples (1) and (5) for further examination. The results of the parameter identification are presented in Table 3, and Figure 6 displays the convergence curves of different algorithms that reflect the objective function value J (Equation 7). It can be seen that IMVO outperforms MVO, PSO, and GA in terms of faster convergence rates. Additionally, it can be observed that the search accuracy of IMVO is superior to the other three algorithms in Cases (1) and (5). Therefore, based on our study, IMVO ranks highest in both convergence rate and search

TABLE 3 The results of identified elastic moduli based on different algorithms.

Method \ Case	Case (1)			Case (5)				
	E'_c (GPa)	E'_r (GPa)	J (mm^2)	E'_c (GPa)	E'_{r1} (GPa)	E'_{r2} (GPa)	E'_{r3} (GPa)	J (mm^2)
IMVO	29.76	19.83	11.9570	30.11	14.75	19.88	24.63	12.5028
MVO	29.78	19.68	11.9575	29.82	14.72	19.68	25.75	12.5116
PSO	29.80	19.38	11.9606	29.07	15.22	18.89	26.36	12.5520
GA	29.62	19.84	11.9573	30.41	14.57	19.47	26.01	12.5265

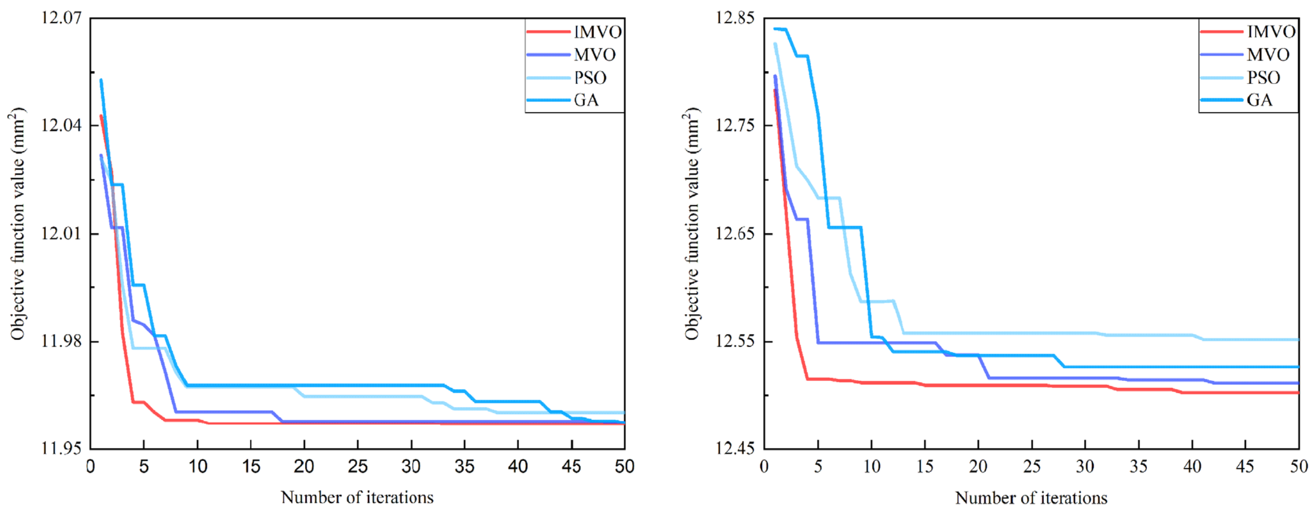

(A) example (1)

(B) example (5)

FIGURE 6 Comparison of convergence curves recorded in the identification process.

capability. Furthermore, the employment of the multi-core parallel computing strategy leads to substantial reductions in computation time. To illustrate, utilizing a quad-core processor for IMVO calculation can save approximately 70% of the time required for the original serial computation because processors can perform calculations simultaneously.

5 | ENGINEERING EXAMPLES

In this section, the feasibility of the proposed stochastic inverse method is examined using a real-world dam project as a case study.

5.1 | Background

A roller compacted concrete dam (RCCD) is located in Southwest China. The non-overflow dam section 11# is selected for analysis. The crest elevation of the dam section is 382.00 m, the foundation surface is 216.43 m, and the crest width is 14 m. There is a folding point located upstream at 270.00 m elevation with a slope of 1:0.25, and the downstream slope is about 1:0.70. The dam body was constructed using concrete material, and according to tests, the density, elastic modulus, Poison ratio, compressive strength and tensile strength are 2.5 g/cm^3, 44.3 GPa, 0.167, 38.55 MPa and 3.39 MPa, respectively. The dam bedrock is mainly composed of sandstone and limestone. The density, elastic modulus, Poison ratio of the bedrock are 2.2 g/cm^3, 30 GPa, and 0.3, respectively.

The dam section is equipped with four plumb lines for monitoring the displacement in the upstream-downstream direction. Three normal plumb lines (PL11-1, PL11-2, and PL11-3) were installed at 379.20, 342.00, and 270.00 m elevations, and PL11-2 has two vertical points (PL11-2-1 and PL11-2-2) at 310.00 and 270.00 m elevations. An inverted plumb line (IP11) was installed at 222.75 m elevation. The plumb line allows for measuring relative displacement between the two ends of the plumb line. For a normal plumb line, the upper end of the wire is fixed at the top of the dam, while a heavy weight is damped at its lower end. For an inverted plumb line, the plumb wire is fixed at the lower end, and the upper end of the

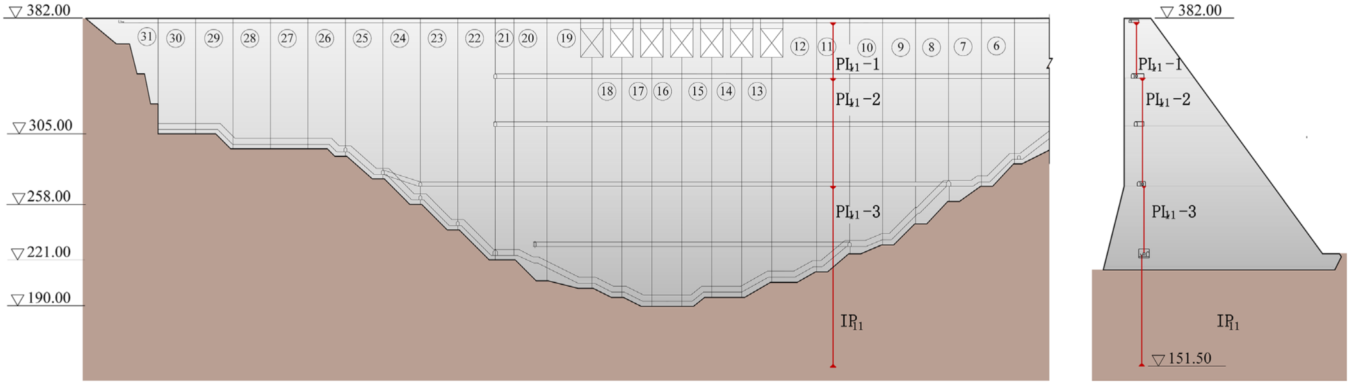

FIGURE 7 Locations of the plumb lines.

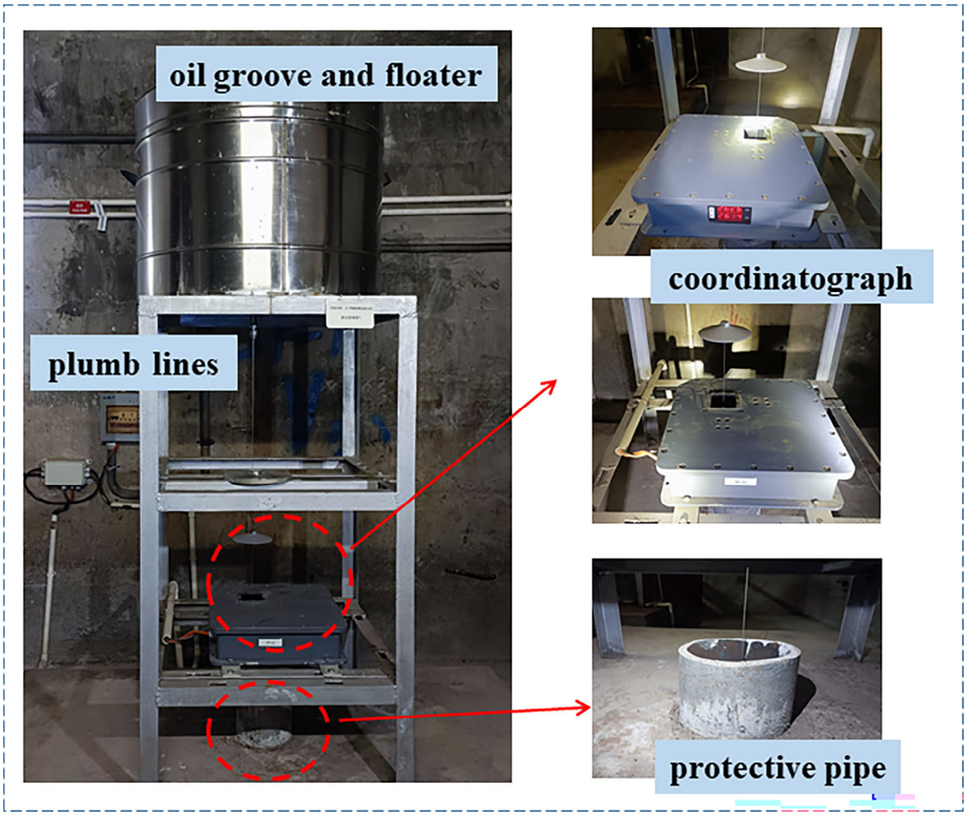

FIGURE 8 The inverted plumb line (IP 11).

wire is linked to a float submerged in a water box in the observation area. The monitoring points in the dam section 11# are shown in Figure 7, and the inverted plumb line (IP11) is illustrated in Figure 8.

5.2 | Statistical analysis

The study period chosen for this study spans from July 28, 2010, to April 15, 2013. Throughout this timeframe, the upstream water level was changed between 334.40 and 369.55 m. The measuring of displacements was conducted twice a month, which resulted in a total of 59 groups of data. By using Equation (29), a statistical model is established for each measuring point allowing for the separation of the hydraulic component, thermal component, and irreversible component. The results of the hydraulic component of the monitoring displacement at different measuring points are presented in Figure 9.

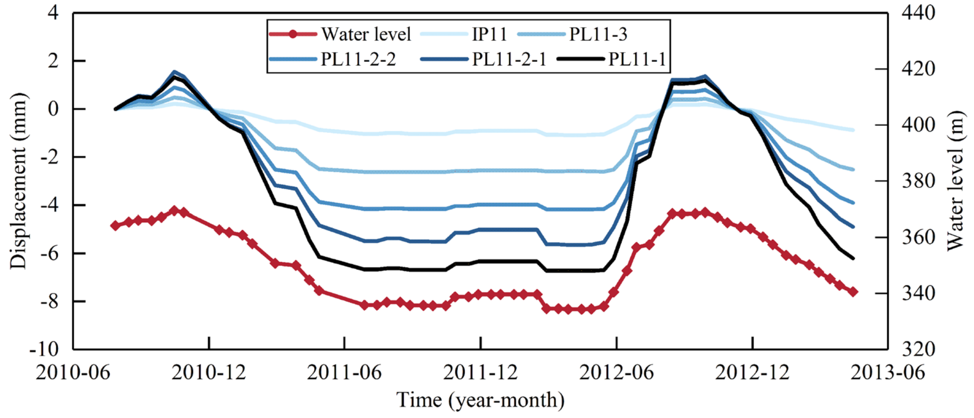

FIGURE 9 The hydraulic component of the monitoring displacement at different measuring points.

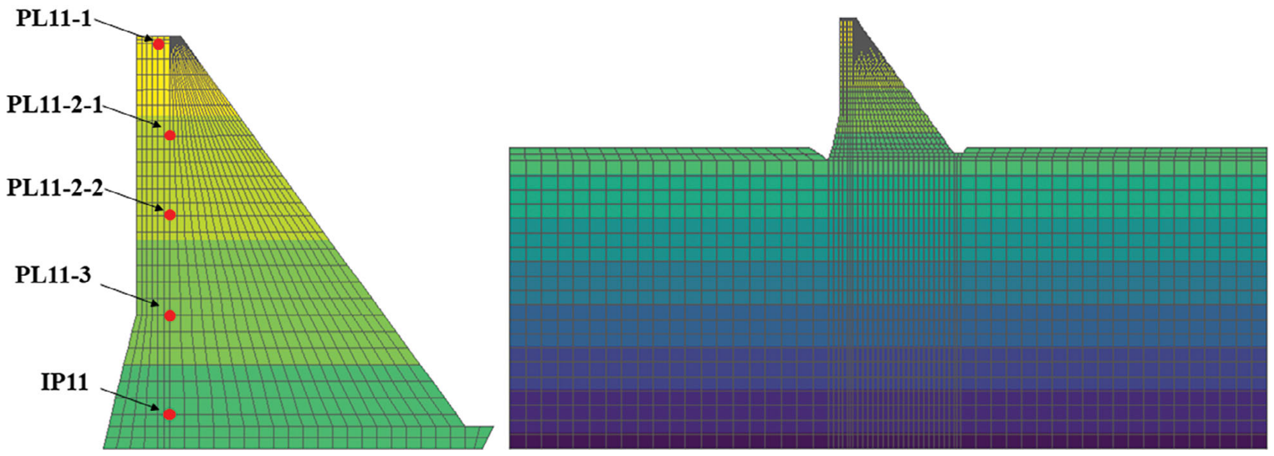

FIGURE 10 FE model for the dam section 11#.

5.3 | Inverse analysis

According to the actual situation of the plumb lines, the FE model of the dam section is established as shown in Figure 10. The FE mesh includes 3736 elements and 3580 nodes. The described model was implemented by GeHoMadrid, a FE program that was jointly developed between Technical University of Madrid (Spain) and Hohai University (China).[50] The program is developed in Fortran and incorporates the PARDISO package for solving highly complicated and sparse equations. It is commonly used to solve complex structural, fluid and multi-physics problems in geotechnical and hydraulic engineering.

In the inverse analysis, the intervals of the elastic moduli of the dam body and foundation are set as $E_c \in [35GPa, 55GPa]$ and $E_r \in [20GPa, 40GPa]$, respectively. Moreover, it has been verified that the load-displacement response of the concrete dam is not significantly influenced by the Poisson ratio, thus the Poisson ratios of the dam body and the foundation are regarded as known and taken as $\mu_c = 0.163$ and $\mu_r = 0.3$, respectively.

After inputting the displacement field data of the five measuring points and the load data into the inverse analysis framework, the elastic moduli of the dam body and foundation can be identified. The identified elastic moduli are expressed in terms of the mean and variance. The mean elastic modulus of the concrete dam body is 45.53 GPa, and its standard deviation is 5.87 GPa resulting in a variation coefficient of 12.9%. This variation coefficient falls within the reasonable range for concrete materials, as reported by Larrard[51] and Vasconcellos.[52] Additionally, the mean elastic modulus of the dam foundation is 31.53 GPa, and its standard deviation is 6.12 GPa resulting in a variation coefficient of 19.4%. It isreasonable that the variation coefficient of bedrock material is higher than that of concrete material.

The statistical results of displacement perturbation terms at different measuring points are shown in Table 4. It is observed that the displacement perturbation caused by stochastic elastic moduli exhibits a mechanically related

TABLE 4 Statistical results of displacement perturbation terms.

Point	IP11	PL11-3	PL11-2-2	PL11-2-1	PL11-1
std(δ'_X) (mm)	0.13	0.28	0.47	0.61	0.81
std(δ'_f) (mm)	0.08	0.09	0.07	0.09	0.07

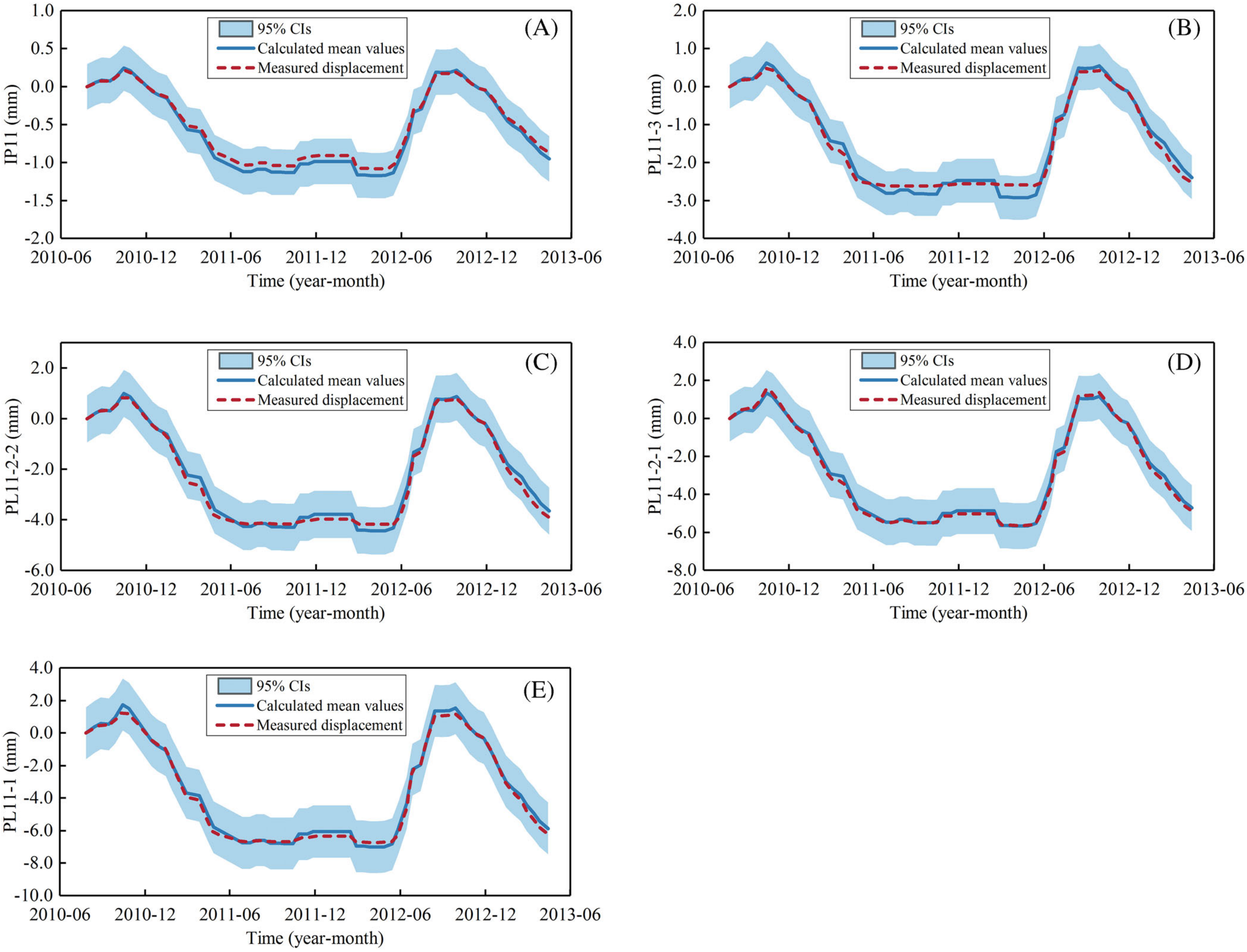

FIGURE 11 The displacement intervals of the measuring points with 95% CIs. (A) IP11, (B) PL11-3, (C) PL11-2-2, (D) PL11-2-1, (E) PL11-1.

phenomenon across different measuring points. Additionally, Table 4 reveals that the observation errors are approximately 0.08 mm.

Based on the analysis above, it is possible to derive a probabilistic output for the dam displacement. The confidence interval (CI) of the displacement can be determined by the statistical variance. For instance, the upper and lower bounds of the 95% CI are defined as $\delta(\overline{X'}, Y) + 1.96 \times \sqrt{\mathrm{var}(\delta'_X) + \mathrm{var}(\delta'_f)}$ and $\delta(\overline{X'}, Y) - 1.96 \times \sqrt{\mathrm{var}(\delta'_X) + \mathrm{var}(\delta'_f)}$, respectively. Figure 11 depicts the displacement intervals of the five measuring points with 95% CIs.

6 | CONCLUSION

This paper presents a novel stochastic inverse method for identifying mechanical parameters of concrete dam system. It involves using reasonable mathematical models and powerful computation tools to analyze the informative content provided by the dam monitoring system. The feasibility of the stochastic inverse method is demonstrated through numerical examples and a practical dam project. The conclusions are as follows:

(1) Based on dam monitoring data, the inversion formulas for unknown stochastic parameters of the dam are derived by combining perturbation equations and Taylor expansion methods. The proposed inverse method allows for the separation of perturbed displacements caused by mechanical parameters from those caused by observation errors. The separated results can effectively reflect the actual working behavior of the dam.
(2) In the inverse analysis framework, the IMVO method is employed to identify the mean of stochastic parameters, while mathematical and statistical methods are used to determine the variance of stochastic parameters. The proposed inverse method has the advantages of simplicity for formulation, efficiency of execution, and ease of understanding.
(3) An IMVO algorithm that combines nonlinear convergence factor strategy and multi-core parallel computing is introduced in the inverse analysis framework. The efficiency of IMVO is confirmed through a comparative study with basic MVO, PSO, and GA.
(4) The current research considers the uncertainty of measurements and materials, the future research will investigate the uncertainty of external loads and other factors comprehensively.

AUTHOR CONTRIBUTIONS

Chaoning Lin: Conceptualization; methodology; software; formal analysis; writing—original draft preparation; funding acquisition. **Xiaohu Du**: Validation. **Siyu Chen**: Software; investigation; data curation; writing—review and editing; visualization; funding acquisition. **Tongchun Li**: Conceptualization; resources; supervision; project administration; funding acquisition. **Xinbo Zhou**: Investigation. **P. H. A. J. M. van Gelder**: Validation; visualization. All of the authors have read and agreed to the published version of the manuscript.

ACKNOWLEDGMENTS

This research was financially supported by the National Key Research and Development Plan of China (No. 2022YFC3005403), National Nature Science Foundation of China (No. 52309151, No. 52309157), the Open Research Fund of Key Laboratory of Reservoir and Dam Safety Ministry of Water Resources (No. YK323007), and the Science and Technology Project of Power Construction Corporation of China (No. DJ-HXGG-2022-02).

DATA AVAILABILITY STATEMENT

The data that support the findings of this study are available on request from the corresponding author. The data are not publicly available due to privacy or ethical restrictions.

ORCID

Chaoning Lin https://orcid.org/0000-0001-5615-308X
Siyu Chen https://orcid.org/0000-0003-1070-9761
Tongchun Li https://orcid.org/0000-0001-6710-5745

REFERENCES

1. Bukenya P, Moyo P, Beushausen H, Oosthuizen C. Health monitoring of concrete dams: a literature review. *J Civ Struct Health Monit*. 2014;4:235-244.
2. Ge W, Li Z, Liang RY, Li W, Cai Y. Methodology for establishing risk criteria for dams in developing countries, case study of china. *Water Resour Manag*. 2017;31:4063-4074.
3. Habib P. The Malpasset dam failure. *Eng Geol*. 1987;24:331-338.
4. Wiley A. The St. Francis dam failure. *J. - Am Water Works Assoc.* 1928;20:338-342.
5. Jia J. A technical review of hydro-project development in China. *Engineering*. 2016;2:302-312.
6. Kao CY, Loh CH. Monitoring of long-term static deformation data of Fei-Tsui arch dam using artificial neural network-based approaches. *Struct Contr Health Monit*. 2013;20:282-303.
7. Li B, Yang J, Hu D. Dam monitoring data analysis methods: a literature review. *Struct Contr Health Monit*. 2019;27:e2501.
8. Hariri-Ardebili MA. Risk, reliability, resilience (R-3) and beyond in dam engineering: a state-of-the-art review. *Int J Disaster Risk Sci*. 2018;31:806-831.
9. Kang F, Liu J, Li J, Li S. Concrete dam deformation prediction model for health monitoring based on extreme learning machine. *Struct Contr Health Monit*. 2017:24: e1997.

10. Su H, Hu J, Wen Z. Structure analysis for concrete-faced rockfill dams based on information entropy theory and finite element method. *Int J Numer Anal Methods Geomech*. 2012;36:1041-1055.
11. Liu G, Xu Y, Wu Z. Total solution for structural mechanics problems. *Comput Methods Appl Mech Eng*. 2001;191:989-1012.
12. Salazar F, Morán R, Toledo MÁ, Oñate E. Data-based models for the prediction of dam behaviour: a review and some methodological considerations. *Arch Comput Meth Eng*. 2017;24:1-21.
13. Salazar F, Toledo MN, González JM, Oate E. Early detection of anomalies in dam performance: a methodology based on boosted regression trees. *Struct Contr Health Monit*. 2017;24:e2012.
14. Hu J, Ma F, Wu S. Comprehensive investigation of leakage problems for concrete gravity dams with penetrating cracks based on detection and monitoring data: a case study. *Struct Contr Health Monit*. 2018;25:e2127.
15. Chen S, Gu C, Lin C, Zhang K, Zhu Y. Multi-kernel optimized relevance vector machine for probabilistic prediction of concrete dam displacement. *Eng Comput*. 2021;37:1943-1959.
16. Kang F, Liu X, Li J. Temperature effect modeling in structural health monitoring of concrete dams using kernel extreme learning machines. *Struct Health Monit*. 2019;19(11):147592171987293.
17. Ribeiro LS, Wilhelm VE, Faria ÉF, Correa JM, Santos ACPD. A comparative analysis of long-term concrete deformation models of a buttress dam. *Eng Struct*. 2019;193:301-307.
18. Marchand B, Chamoin L, Rey C. Parameter identification and model updating in the context of nonlinear mechanical behaviors using a unified formulation of the modified constitutive relation error concept. *Comput Methods Appl Mech Eng*. 2019;345:1094-1113.
19. Jiang Q, Sun Y, Yi B, Li T, Xiong F. Inverse analysis for geomaterial parameter identification using Pareto multiobjective optimization. *Int J Numer Anal Methods Geomech*. 2018;42:1698-1718.
20. Abreu R, Mejía C, Roehl D. Inverse analysis of hydraulic fracturing tests based on artificial intelligence techniques. *Int J Numer Anal Methods Geomech*. 2022;46:2582-2602.
21. Lin C, Li T, Chen S, Yuan L, van Gelder P, Yorke-Smith N. Long-term viscoelastic deformation monitoring of a concrete dam: a multi-output surrogate model approach for parameter identification. *Eng Struct*. 2022;266:114553.
22. Lin C, Li T, Chen S, et al. Structural identification in long-term deformation characteristic of dam foundation using meta-heuristic optimization techniques. *Adv Eng Software*. 2020;148:102870.
23. Ardito R, Bartalotta P, Ceriani L, Maier G. Diagnostic inverse analysis of concrete dams with statical excitation. *J Mech Behav*. 2011;15:381-390.
24. De Sortis A, Paoliani P. Statistical analysis and structural identification in concrete dam monitoring. *Eng Struct*. 2007;29:110-120.
25. Yang L, Su H, Wen Z. Improved PLS and PSO methods-based back analysis for elastic modulus of dam. *Adv Eng Software*. 2019;131:205-216.
26. Kang F, Liu X, Li J, Li H. Multi-parameter inverse analysis of concrete dams using kernel extreme learning machines-based response surface model. *Eng Struct*. 2022;256:113999.
27. Hariri-Ardebili M, Seyed-Kolbadi S, Saouma V, Salamon J, Rajagopalan B. Random finite element method for the seismic analysis of gravity dams. *Eng Struct*. 2018;171:405-420.
28. Soltani N, Alembagheri M, Khaneghahi MH. Risk-based probabilistic thermal-stress analysis of concrete arch dams. *Front Struct Civ Eng*. 2019;13:1007-1019.
29. Conde B, Eguía P, Stavroulakis GE, Granada E. Parameter identification for damaged condition investigation on masonry arch bridges using a Bayesian approach. *Eng Struct*. 2018;172:275-284.
30. Chen B, Zhao H, Ru Z, Li X. Probabilistic back analysis for geotechnical engineering based on Bayesian and support vector machine. *J Cent South Univ*. 2015;22:4778-4786.
31. Chen Y, Lu Z, Yang Z, Ke L. Parameter identification for structural dynamics based on interval analysis algorithm. *Acta Astronaut*. 2018;145:131-140.
32. Cornell CA. 1971:130-144.
33. Nayfeh AH. *Perturbation Methods*. Wiley; 1973.
34. Henriques AA. Efficient analysis of structural uncertainty using perturbation techniques. *Eng Struct*. 2008;30:990-1001.
35. Kleiber M, Tran DH. *The Stochastic Finite Element Method: Basic Perturbation Technique and Computer Implementation*. John Wiley and Sons; 1992.
36. Mellah R, Auvinet G, Masrouri F. Stochastic finite element method applied to non-linear analysis of embankments. *Probab Eng Mech*. 2000;15:251-259.
37. Kaminski M. On the generalised perturbation-based stochastic finite element method. Proceedings of the 7th International Conference on Computational Structural Technology, Civil-Comp Press, Stirling, Scotland; 2004.
38. Lofrano E, Paolone A, Vasta M. A perturbation approach for the identification of uncertain structures. *Int J Dyn Contr*. 2016;4:204-212.
39. Mirjalili S, Mirjalili SM, Hatamlou A. Multi-verse optimizer: a nature-inspired algorithm for global optimization. *Neural Comput Appl*. 2016;27:495-513.
40. Abualigah L. Multi-verse optimizer algorithm: a comprehensive survey of its results, variants, and applications. *Neural Comput Appl*. 2020;32:12381-12401.
41. Aljarah I, Mafarja M, Heidari AA, Faris H, Mirjalili S. Multi-verse optimizer: theory, literature review, and application in data clustering. *Nature-Inspired Optimizers: Theories, Literature Reviews and Applications*. Springer; 2020:123-141.
42. Ewees AA, El Aziz MA, Hassanien AE. Chaotic multi-verse optimizer-based feature selection. *Neural Comput Appl*. 2019;31:991-1006.

43. Farahmand-Tabar S, Babaei M. Memory-assisted adaptive multi-verse optimizer and its application in structural shape and size optimization. *Soft Computing*. 2023;27:11505-11527.
44. Abualigah L, Alkhrabsheh M. Amended hybrid multi-verse optimizer with genetic algorithm for solving task scheduling problem in cloud computing. *J Supercomput*. 2022;78:740-765.
45. Makhadmeh SN, Abasi AK, Al-Betar MA. Hybrid multi-verse optimizer with grey wolf optimizer for power scheduling problem in smart home using IoT. *J Supercomput*. 2022;78:11794-11829.
46. Li M, Shen Y, Ren Q, Li H. A new distributed time series evolution prediction model for dam deformation based on constituent elements. *Adv Eng Inf*. 2019;39:41-52.
47. Li M, Wang J. An empirical comparison of multiple linear regression and artificial neural network for concrete dam deformation modelling. *Math Probl Eng*. 2019.
48. Kang F, Li JJ, Zhao SZ, Wang YJ. Structural health monitoring of concrete dams using long-term air temperature for thermal effect simulation. *Eng Struct*. 2019;180:642-653.
49. Lin C, Li T, Chen S, Liu X, Lin C, Liang S. Gaussian process regression-based forecasting model of dam deformation. *Neural Comput Appl*. 2019;31:8503-8518.
50. Fernandez-Merodo JA, Castellanza R, Mabssout M, Pastor M, Parma M. Coupling transport of chemical species and damage of bonded geomaterials. *Comput Geotech*. 2007;34:200-215.
51. De Larrard T, Colliat JB, Benboudjema F, Torrenti JM, Nahas G. Effect of the Young modulus variability on the mechanical behaviour of a nuclear containment vessel. *Nucl Eng Des*. 2010;240:4051-4060.
52. de Vasconcellos Real M, Campos Filho A, Maestrini SR. Response variability in reinforced concrete structures with uncertain geometrical and material properties. *Nucl Eng Des*. 2003;226:205-220.

How to cite this article: Lin C, Du X, Chen S, Li T, Zhou X, Gelder PHAJM. On the multi-parameters identification of concrete dams: A novel stochastic inverse approach. *Int J Numer Anal Methods Geomech*. 2024;1-19. https://doi.org/10.1002/nag.3812